Graphene on Ru(0001): Evidence for two graphene band structures

Khabibulakh Katsiev, Yaroslav Losovyj, Zihao Zhou, Elio Vescovo, Li Liu, Peter A. Dowben, and D. Wayne Goodman

Phys. Rev. B **85**, 195405 — Published 3 May 2012

DOI: 10.1103/PhysRevB.85.195405

Graphene on Ru(0001): Evidence for Two Graphene Band Structures

Khabibulakh Katsiev[1], Yaroslav Losovyj[2], Zihao Zhou[1], Elio Vescovo[3], Li Liu[1], P. A. Dowben[4], and D. Wayne Goodman[1]

[1] Department of Chemistry, Texas A&M University, College Station TX 77842

[2] The J. Bennett Johnston Sr. Center for Advanced Microstructures and Devices, Louisiana State University, 6980 Jefferson Hwy., Baton Rouge LA 70806

[3]National Synchrotron Light Source, Brookhaven National Laboratory, Upton, New York 11973, USA

[4]Department of Physics and Astronomy, University of Nebraska, Theodore Jorgensen Hall, 855 North 16th Street, P.O. Box 880299, Lincoln, NE 68588-0299, USA

Abstract: High resolution photoemission illustrates that the band structure of graphene on Ru(0001) exhibits a well defined splitting. This splitting is largest with the graphene directly on the Ru(0001) substrate whereas with a chemisorbed oxygen spacer layer between the graphene and the metal substrate, this splitting is considerably reduced. This splitting is attributed to a combination of chemical interactions between graphene and Ru(0001) and to screening of the former by the latter, not spin-orbit coupling.

Keywords: Symmetry reduction, substrate interactions, graphene
PACS Numbers: 71.20.-b 79.60.-I, 71.20.Tx, 73.20.-r, 73.22.Gk

I. INTRODUCTION

Graphene grown on single crystal substrates like Ru(0001) is extremely ordered [1-10], but characterized by two chemically different species [2-9]. This has usually been ascribed to a rumpling of the graphene overlayer, thus there would be patches of graphene strongly hybridized with the substrate and regions where such hybridization is weak [7,10,11]. In the regions with a strong interaction there is charge transfer and the possible opening of a band gap [7,10]. If the rumpling occurs without grain boundaries, one might suspect a continuum graphene – substrate hybridization from strong (close proximity) to weak (separation from the substrate). Either a continuum of graphenes or small patches of graphene in the strong and weak substrate hybridization regime would lead to a smearing of the valence band structure [12]. If the graphene in one chemical regime or the other is large enough in spatial extent, then wave vector conservation in the plane of the graphene remains preserved with very high fidelity, and two distinct band structures may emerge, as is suggested by spatially resolved STM spectroscopy studies [4]. But strong interactions with the substrate can also lift the chemical degeneracy of the A and B graphene sites, reducing the symmetry to C_3 and opening up a band gap in the graphene [13,14].

Splitting of the graphene bands for graphene on Ru(0001) could also arise from several effects. The splitting could be a result of spin orbit effects as is observed for paramagnetic metals surfaces [15-18]. For graphene on a metal substrate, however, there is a loss of inversion symmetry along the surface normal as well as in the plane of the film, therefore the spin orbit coupling splitting for graphene should be very small (~10 μeV or less) [19-23]. While the substrate can alter the spin orbit coupling significantly [24], this is unlikely to be the case for graphene [15], because of the low Z of carbon.

Other possibilities for splitting of the graphene valence band include a chemical shift between the top layer of graphene and the layer in intimate contact with the substrate as has been proposed for the "split" valence band structure of graphene on Ru(0001) [25] and SiC [26]. The Moiré resulting from the overlaid graphene and the Ru(0001) surface also leads to a supercell that can give rise to Dirac cone replicas, as seen for graphene Ru(0001) [10] and Ir(111) [27].

II. EXPERIMENTAL

The STM experiments were carried out in the ultrahigh vacuum (UHV) chamber with the base pressure ~$1x10^{-10}$ Torr. The chamber was equipped with room temperature scanning tunneling microscope (STM) Omicron STM-1, a cylindrical mirror energy analyzer for Auger electron spectroscopy (AES), low energy electron diffraction (LEED) optics, as detailed elsewhere [28]. All STM images were acquired in the constant-current mode with an electrochemically etched W tip. The bias voltages are reported with reference to the sample.

The angular resolved photoemission spectroscopy (ARPES) studies were acquired at the U5UA undulator spherical grating monochromator (SGM) beamline at the National Synchrotron Light Source (NSLS) [29,30]. An angle-resolved hemispherical electron energy analyzer (EA125, Omicron GmbH) was used for these experiments [30]. The light was incident at 45° from the sample normal and the photon energy was 45 eV for the data presented, unless stated otherwise, although data were collected at a variety of photon energies. The typical overall instrumental resolution was approximately 80 meV (spin integrated).

The Ru(0001) substrate was cleaned by cycles of Ar ion sputtering, annealing in $1.0x10^{-7}$ Torr of O_2 at~1100 K, and flashing to 1800 K in vacuum. The surface cleanness was monitored by AES (not shown), LEED (Fig. 1D), and, where available, STM (Fig. 1A). Single-layer graphene was formed by first exposing a clean (metallic) Ru(0001) sample to ethylene or propylene with a pressure of 1 x 10^{-7} Torr at room temperature, followed by annealing the sample to 1300K, and then slowly cooling to 1000 K. This process was repeated several times in order to synthesize graphene that uniformly covered the Ru(0001) substrate. The quality of the graphene overlayer was monitored by LEED (Fig. 1E). Due to the lattice mismatch between graphene and the surface of Ru(0001), a Moiré structure was formed, as shown in the low energy electron diffraction of Fig. 1E, with a superstructure lattice constant of ~3.0 nm [2], as shown in Fig. 1B. It is noteworthy, however, that there is no evidence of a reduction of symmetry due to an inequivalence in the graphene A and B sites as noted elsewhere for graphene on other substrates [10,31].

Graphene on the oxidized Ru(0001) surface was prepared by first growing single-layer graphene, then oxidizing the Ru surface by heating the sample to ~700 K in 1 x 10^{-7} Torr of oxygen for 5 minutes. This procedure results in the formation of the Ru(0001)(2 x 2) surface oxide structure (as seen in the LEED of Fig. 1F) [3] with strong suppression of the Moiré as seen in the LEED of the graphene overlayer. As seen in the STM image of Fig. 1C, the graphene overlayer is less corrugated with no evidence of a Moiré structure.

III. RESULTS AND DISCUSSION

The band structure of monolayer graphene on Ru(0001), with well defined bands along $\overline{\Gamma}$-$\overline{K}$, is shown in Figs. 2B and 2C. The fact that the graphene is not in registry with the substrate suggests that the graphene band structure is decoupled from the substrate and that the Brillouin zone edge along $\overline{\Gamma}$-$\overline{K}$ occurs at 1.7 $Å^{-1}$ (as seen in Fig. 2), consistent with graphene, not Ru(0001) [11]. The band structure exhibits a clear splitting of the bands associated with the graphene overlayer, as seen along both $\overline{\Gamma}$-$\overline{K}$, as illustrated in Fig. 2. This splitting of the graphene bands occurs not only in the region of the Fermi level, but also well away from the Fermi level along $\overline{\Gamma}$-$\overline{K}$, as seen in Fig. 2. Such a splitting of bands over such large regions of k-space tends to exclude an origin that is related to spin-orbit splitting, since such surface or overlayer Rashba interactions are expected to be wave vector dependent and the two spin-split bands must be degenerate at k = 0 (i.e. at $\overline{\Gamma}$). Furthermore, the band splitting for graphene on Ru(0001) even exceeds the spin-orbit splitting of more than 500 meV reported for the hydrogen-covered W(110) surface states near E_F [32,33]. It is noteworthy that this magnitude of splitting is not seen for graphene on gold on Ru(0001) [34] where one might expect spin-orbit coupling because of interactions with the higher Z of gold [15]. The splitting also cannot be attributed to "shadow" bands due to the Moiré multiple diffraction effects reported elsewhere for graphene on Ru(0001) [10] and Ir(111) [26], because the splitting is seen well away from the Fermi level with significant intensity in both components. Thus, with the exclusion of spin-orbit splitting and Moiré related shadow bands, the observed splitting of the band structure suggests two chemically distinct states of graphene.

It can be argued that the observed splitting of the π-band is due to the formation of multilayer graphene, where the first monolayer of graphene, that couples strongly with the Ru substrate, and patches or/and overlayers of freestanding double- or triple-layered graphene, that couple less strongly, form two distinct bands. This is not the case in our experiments, because the well-defined Dirac cone at the $\overline{\Gamma}$-$\overline{K}$ point, indicative of free-standing, multilayer graphene or multilayer graphene on Ru(0001) is absent [25]. As shown in the supplementary material, the photoemission intensity is illustrative of an incomplete Dirac cone and asymmetric about the $\overline{K}$ point near the Fermi level (supplementary material; Fig. S1), completely consistent with prior studies of monolayer graphene on Ru(0001) [11]. Only for bilayer graphene on Ru(001) does the π-band of graphene extend to the $\overline{K}$ point [25]. Furthermore, the measured work function of Ø = 4.2 eV for the graphene/Ru(0001) system is also in a good agreement with that reported in the literature for single-layer graphene on Ru [11]. Furthermore, for a graphene bilayer on SiC, the splitting of the graphene band structure, resulting from the chemical inequivalence two graphene layers with respect to charge and electrostatic potential, leads to a splitting of the band structure becomes less distinct at smaller wave vectors, towards the surface Brillouin zone center, at increasing binding energies away from the Fermi level [26].

As mentioned above, oxygen exposure to graphene on Ru(0001) yields a graphene layer on an oxygen layer chemisorbed on Ru(0001). This should change the graphene Ru(0001) interaction significantly. Graphene on Ru(0001) should acquire charge of about 0.05 e^- per carbon atom [10,11,25,30], while graphene on chemisorbed oxygen on Ru(0001) should be slightly electron deficient. As seen in a comparison of Fig. 2B with Fig. 2C, there are distinct changes in the band structure. Key among these changes observed in the graphene overlayer band structure is not just simply a shift in the binding energies of the various graphene bands but also a splitting of the graphene bands. There is a decrease in the splitting of the graphene bands in the region along $\overline{\Gamma}$-$\overline{K}$, from ~800 meV to ~400 meV, with insertion of a chemisorbed oxygen interlayer between the Ru(0001) and the graphene. This correlates with the morphological changes in the graphene overlayer on Ru(0001) observed with STM subsequent to oxygen exposure. After the oxygen exposure, the corrugation of the graphene overlayer becomes significantly smaller compared to that of graphene on metallic Ru(0001), with a peak-to-valley corrugation estimated to be 0.1 and

0.03 nm for the graphene on metallic and oxidized Ru(0001), respectively. In addition, the graphene band structure is illustrative of a more complete Dirac cone, as would be expected if the graphene more closely resembled a free-standing graphene layer [35].

The monolayer graphene band structure data indicate that the splitting of the graphene band structure is characteristic of a difference in the chemical potential "felt" by the graphene overlayer, and not an effect of spin-orbit splitting. The splitting of the graphene band structure observed here for graphene on Ru(0001) is larger than the splitting of graphene bilayers [25,26], some 800 meV instead of the expected 400 meV. Although the monolayer graphene monolayer on Ru(0001) is observed to separate into two chemically different species [2-9], other factors also play a role, among which is that the rumpling of the monolayer renders patches of the graphene layer inequivalent with respect to charge [36], based on the core level binding energy shifts [37], as well inequivalent with respect to the electrostatic potential and in terms of the substrate screening the photoemission final state [38]. These inequivalencies all contribute to an increase in the apparent splitting of the graphene band structure well beyond that expected by charge displacement [38], and these inequivalencies are reduced by the insertion of oxygen between the graphene and the substrate.

Recent work suggests that the screening of a dipole adsorbate on graphene is very different from that of other very good conductors, even considering the differences in carrier densities in graphene (due to the dimensionality restrictions) with those of metal surfaces. This can lead to the binding energy shifts seen in photoemission [35,38]. This means that binding energy shifts in the valence band spectra are significantly larger for screened and unscreened graphene, due to the rumpling of the graphene sheet. These apparent shifts in the graphene spectra should be much larger than those observed with other adsorbates on Ru(0001). Furthermore, there is a large body of theory indicating that such binding energy shifts in the valence band, as a result of the differences in the electrostatic potential and adsorbate graphene hybridization [38] (as well as the substrate screening the photoemission final state) are not only possible, but indeed likely. Of course distinguishing between initial state effects such as charge transfer to the graphene and final state effects due to screening in the proximity of a metal substrate, for example, is difficult.

If chemisorbed oxygen is then placed between the graphene and the Ru(0001), the surface of the substrate is no longer fully metallic. A graphene layer on a chemisorbed oxygen layer should, in principle, be more weakly coupled to the substrate. This weaker interaction would cause a shift of the graphene band structure, a loss of the Moiré in the LEED, and a decrease in the graphene atomic corrugation. Perhaps more importantly, the expected, but not previously reported, splitting of the graphene bands should decrease, as is observed (Figs. 2D and 2E). In this context, the hybridization with the substrate must be re-examined. If the two different graphene band structures are to be explained to be a direct consequence of the rumpling or corrugation of the graphene such that certain areas are in close proximity to the metal substrate and other areas are displaced from the substrate, certain requirements must be met. The graphene in one of these chemical regimes must be sufficiently spatially extensive such that wave vector conservation in the plane of the graphene remains preserved with sufficient fidelity that two distinct band structures may emerge, as is suggested by spatially resolved STM studies [4]. Any smoothly undulating potential (with no large areas of chemical equivalence) would not, by itself, explain the two distinct band structures.

Performing experiments with oxygen placed between the Ru(0001) and the graphene provides evidence that the shift of the band is due primarily to screening (final state) effects. With uniform oxygen chemisorption between the metal substrate surface and the graphene film, there is a global "relaxation" of the rumpling or long range variations in the displacement of the graphene relative to the substrate while graphene hybridization with the substrate is weakened. Because of the variations in the displacement of the graphene relative to the substrate that remain after insertion of the oxygen spacer layer, the graphene band structure should remain "split" but with a diminished splitting, as is observed (Figs. 2D and 2E). Because these are band structure effects consistent with the band structure of graphene, the two chemical states are not the result of short range effects, such as a broken graphene A/B carbon symmetry due to a strong interaction with the Ru(0001) metal substrate. The latter is not evident in STM. Any initial chemical state differences between the A/B sites would be very much suppressed along the $\overline{\Gamma}$-$\overline{\mathrm{K}}$ high symmetry direction, as differences between the A/B graphene sites would reduce the surface symmetry to C_{3v} [13]. In C_{3v}, the $\overline{\mathrm{K}}$ high symmetry point reflects the k-space point with no mirror

inversion symmetry. The absence of registry with the substrate and the C_{6v} symmetry of the LEED and the STM (Fig. 1) exclude a chemical inequivalence of the graphene A and B sites, though this might exist on an oxide surface [13]. The potential differences due to the rumpling of graphene on Ru(0001) are seen not just in the spatially resolved electronic structure [4], the Xe $5p_{1/2}$ binding energies [11], and the C 1s core level spectra [38], but in the formation of two distinct graphene band structures. The two chemical regimes for graphene on Ru(0001) are large enough in spatial extent that wave vector conservation in the plane of the graphene remains preserved with very high fidelity along the $\overline{\Gamma}$-$\overline{K}$ high symmetry direction. This is consistent with the two distinct core levels measured for single layer graphene on Ru(0001) [37], with a core level splitting of 600 meV, similar to the splitting of the two chemically inequivalent graphene valence band structures presented here.

ACKNOWLEDGEMENTS

This material is based upon work supported as part of the Center for Atomic-Level Catalyst Design, an Energy Frontier Research Center funded by the U.S. Department of Energy, Office of Science, Office of Basic Energy Sciences under Award Number #DE-SC0001058. The NSLS is supported by the United States Department of Energy, Office of Science, Office of Basic Energy Sciences, under Contract No. DE-AC02-76CH00016. The J. Bennett Johnston Sr. Center for Advanced Microstructures and Devices is supported by the Louisiana Board of Regents. The work at UNL was supported by the Semiconductor Research Corporation, Division of Nanomanufacturing Sciences administered by Boyan Boyanov and Bob Havemann under Task ID 2123.001. The authors acknowledge helpful conversations with Jeff Kelber, Wai-Ning Mei and Lingmei Kong.

References:

[1] Z. Zhou, F. Gao, and D.W. Goodman, Surf. Sci. **604,** L31 (2010).

[2] S. Marchini, S. Günther, and J. Wintterlin, Phys. Rev. B **76**,075429 (2007).

[3] Y . Pan, D-X. Shi, and H.-J. Gao, Chinese Phys. **16,** 3151 (2007).

[4] A. L. Vàzquez de Parga, F. Calleja, B. Borca, M. C. G. Passeggi, J. J. Hinarejos, F. Guinea, and R. Miranda, Phys. Rev. Lett. **100,** 056807 (2008).

[5] D.Martoccia, P.R. Willmott, T. Brugger, M. Bjoerck, S. Guenther, C.M. Schlepuetz, A. Cervellino, S.A. Pauli, B. D. Patterson, S. Marchini, J. Wintterlin, W. Moritz, and T. Greber, Phys. Rev. Lett. **101,** 126102 (2008).

[6] Y.Pan, H. Zhang, D. Shi, J. Sun, S. Du, F. Liu, and H.Gao, Adv. Mater. **21,** 2777 (2009).

[7] B.Wang, M. L. Bocquet, S. Marchini, S . Günther, and J. Wintterlin, Phys. Chem. Chem. Phys. **10**, 3530 (2008).

[8] D. E. Jiang, M. H. Du, and S .Dai,J. Chem. Phys. **130**, 074705 (2009).

[9] D. Martoccia, M. Björck, C.M. Schlepütz, T. Brugger, S.A. Pauli, B.D. Patterson, T. Greber, and P.R. Willmott, New J. Phys.**12**, 043028 (2010).

[10] E. Sutter, D. P. Acharya, J. T. Sadowski, and P. Sutter, Appl. Phys. Lett. **94** 133101 (2009).

[11] T.Brugger, S. Günther, B. Wang, J. Hugo Dil, M-L. Bocquet, J. Osterwalder, J. Wintterlin, and T. Greber, Phys. Rev. B**79,** 045407 (2009).

[12] A.Isacsson, L. M. Jonsson, J. M. Kinaret, and M. Jonson, Phys. Rev. B **77**, 035423 (2008).

[13] S. Gaddam, C. Bjelkevig, S. Ge, K. Fukutani, P. A. Dowben, J.A. Kelber, J. Phys.: Condens. Matter **23,** 072204(2011).

[14] Zhou *et al*., Nat. Mat. **6**, 770 (2007).

[15] E. E. Krasovskii and E. V. Chulkov, Phys. Rev. B **83,** 155401 (2011).

[16] J. I. Pascual *et al*, Phys. Rev. Lett. **93**, 196802 (2004).

[17] J. H. Dil, J. Phys.: Condens. Matter **21**, 403001 (2009)

[18] K. Sakamoto*et al*, Phys. Rev. Lett. **103**, 156801 (2009).

[19] D. Huertas-Hernando, F. Guinea, and A. Brataas, Phys. Rev. B **74**, 155426 (2006).

[20] H. Min *et al*., Phys. Rev. B **74**, 165310 (2006).

[21] Y. Yao*et al*., Phys. Rev. B **75**, 041401(R) (2007).

[22] B. Trauzettel*et al*., Nat. Phys. **3**, 192 (2007).

[23] D. Huertas-Hernando, F. Guinea, and A. Brataas, Phys. Rev. Lett. **103**, 146801 (2009).

[24] E. Rotenberg, J.W. Chung and S.D. Kevan, Phys. Rev. Lett. **82,** 4066 (1999).

[25] P. Sutter, M. S. Hybertsen, J. T. Sadowski, and E. Sutter, Nano Lett. **9,** 2654 (2009).

[26] T. Ohta, A. Bostwick, T. Seyller, K. Horn, E. Rotenberg, Science **313**, 951 (2006)

[27] I. Pletikosic´, M. Kralj, P. Pervan, R. Brako, J. Coraux, A. T. N'Diaye, C. Busse, and T. Michely, Phys. Rev. Lett. **102,** 056808 (2009).

[28] X. Lai, T.P. St. Clair, M. Valden, and D.W. Goodman, Prog. Surf. Sci. **59,** 25 (1998).

[29] E. Vescovo*et al*., U5UA: Synch. Rad. News**12,** 10 (1999).

[30] D.D. Neufeld, H. Aliabadi, and F.B. Dunning, Rev. Sci. Instrum. **78**, 25107 (2007).

[31] L. Kong et al., J. Phys. Chem. **114,** 21618 (2010).

[32] M. Hochstrasser, J. G. Tobin, E. Rotenberg and S. D. Kevan, Phys. Rev. Lett. **89,** 216802 (2002).

[33] A. Eiguren and C. Ambrosch-Draxl, New J. Phys. **11,** 013056 (2009).

[34] C. Enderlein, Y. S. Kim, A. Bostwick, E. Rotenberg, and K. Horn, New J. Phys. **12,** 033014 (2010).

[35] L. Kong, et al., Carbon **50,** 1981 (2012)

[36] U. Gelius, Physica Scripta **9**, 133 (1974)

[37] A. B. Preobrajenski, May Ling Ng, A. S. Vinogradov, N. Mårtensson, Phys. Rev. B **78**, 073401 (2008)

[38] J.M. Garcia-Lastra, C. Rostgaard, A. Rubio, K.S. Thygesen, Phys. Rev. B **80**, 245427 (2009).

Figure Captions

Figure 1: (A) Room temperature UHV STM image of a clean Ru(0001) surface (200x200nm^2, V_{sample} 1V, $I_{tunneling}$ 100pA); (B) graphene on Ru(0001) (100x100nm^2, V_{sample} 0.1V, $I_{tunneling}$ 200pA); (C) graphene on oxidized Ru(0001) (4x4 nm^2, V_{sample} 0.3V, $I_{tunneling}$ 300pA); (D-F) corresponding LEED patterns of clean Ru(0001), graphene on Ru(0001), and graphene on an oxidized Ru(0001) surface, respectively (color online).

Figure 2. ARUPS spectra (acquired at 45eV photon energy along the $\overline{\Gamma}$-$\overline{K}$ direction) of: (A) clean Ru (0001); (B) graphene/Ru(0001); (C) high resolution map of the graphene band region indicated by the white dashed rectangle in (B); (D) graphene/oxidized Ru(0001); (E) high resolution map of the graphene band region indicated by the white dashed rectangle in (D)(color online).

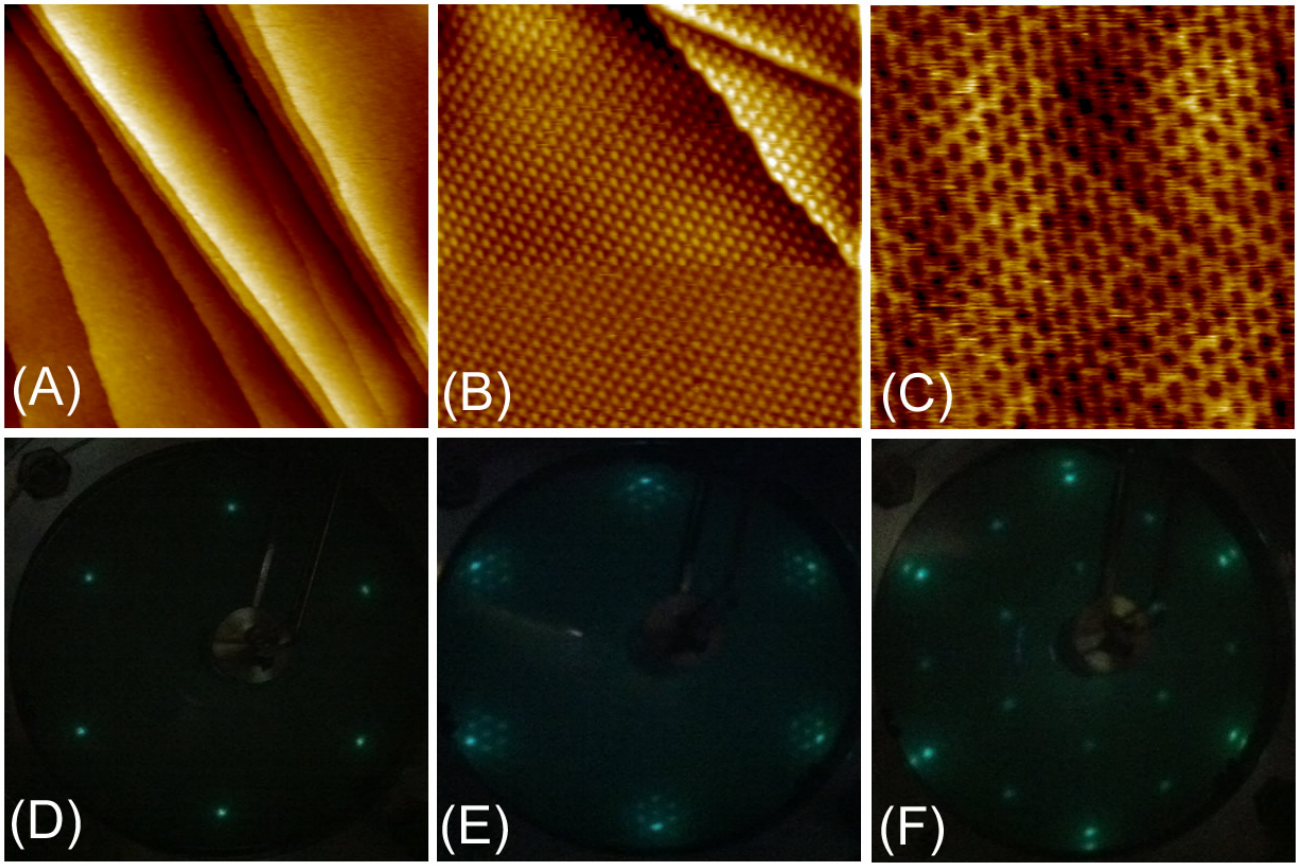

Figure 1

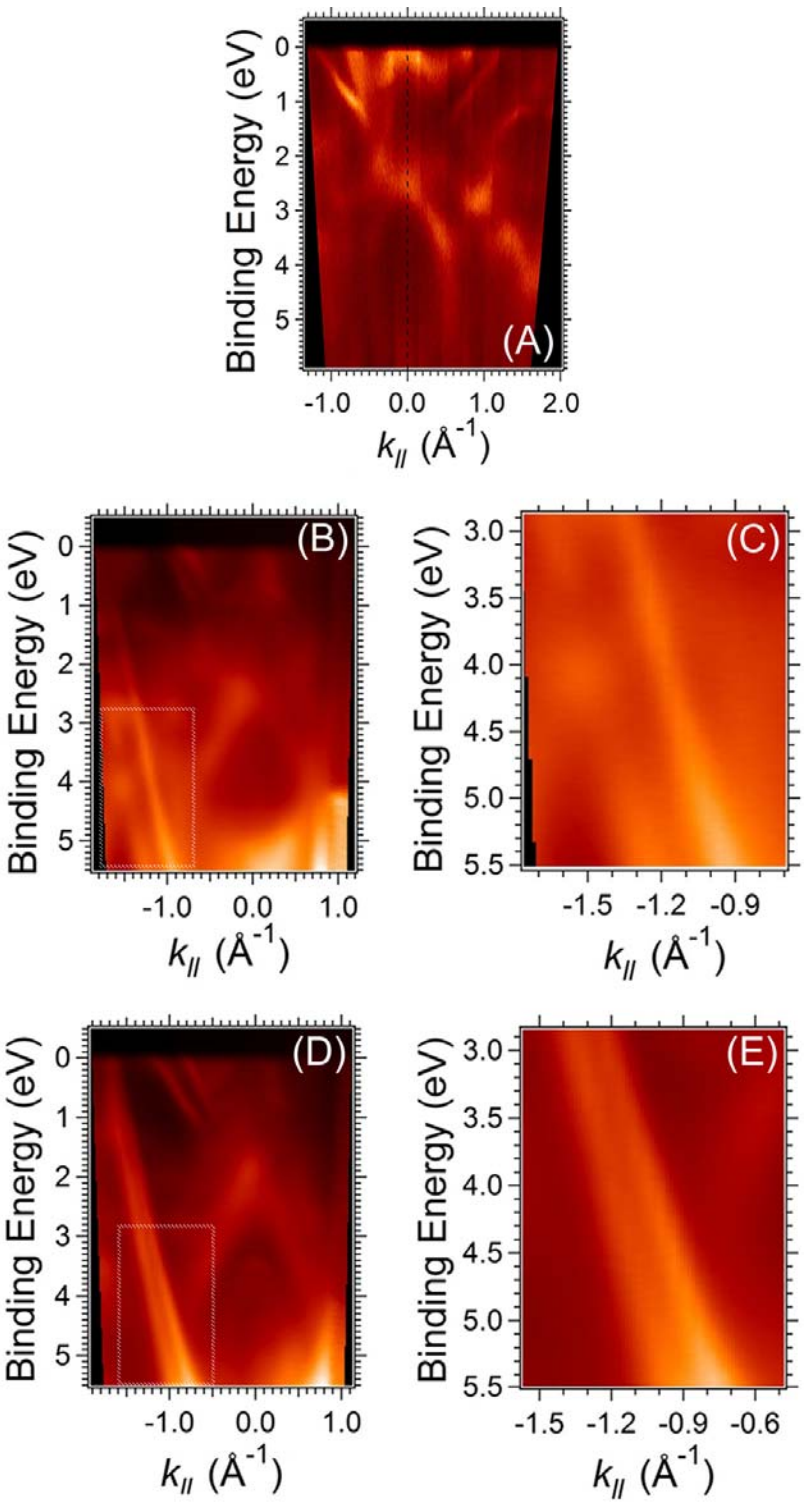
(A)
Binding Energy (eV)
0
1
2
3
4
5
-1.0
0.0
1.0
2.0
$k_{//}$ (Å^{-1})
(B)
Binding Energy (eV)
0
1
2
3
4
5
-1.0
0.0
1.0
$k_{//}$ (Å^{-1})
(C)
Binding Energy (eV)
3.0
3.5
4.0
4.5
5.0
5.5
-1.5
-1.2
-0.9
$k_{//}$ (Å^{-1})
(D)
Binding Energy (eV)
0
1
2
3
4
5
-1.0
0.0
1.0
$k_{//}$ (Å^{-1})
(E)
Binding Energy (eV)
3.0
3.5
4.0
4.5
5.0
5.5
-1.5
-1.2
-0.9
-0.6
$k_{//}$ (Å^{-1})

Figure 2